Hindawi Publishing Corporation
Mathematical Problems in Engineering
Volume 2010, Article ID 909240, 15 pages
doi:10.1155/2010/909240

Research Article

Optimization Shape of Variable Capacitance Micromotor Using Differential Evolution Algorithm

A. Ketabi[1] and M. J. Navardi[2]

[1] *Department of Electrical Engineering, University of Kashan, Kashan 87317- 51167, Iran*
[2] *Department of Electrical Engineering, I.A.U.-Kashan Branch, Kashan 87317-51290, Iran*

Correspondence should be addressed to A. Ketabi, aketabi@kashanu.ac.ir

Received 23 May 2010; Revised 9 November 2010; Accepted 29 November 2010

Academic Editor: Mohammad Younis

A new method for optimum shape design of variable capacitance micromotor (VCM) using Differential Evolution (DE), a stochastic search algorithm, is presented. In this optimization exercise, the objective function aims to maximize torque value and minimize the torque ripple, where the geometric parameters are considered to be the variables. The optimization process is carried out using a combination of DE algorithm and FEM analysis. Fitness value is calculated by FEM analysis using COMSOL3.4, and the DE algorithm is realized by MATLAB7.4. The proposed method is applied to a VCM with 8 poles at the stator and 6 poles at the rotor. The results show that the optimized micromotor using DE algorithm had higher torque value and lower torque ripple, indicating the validity of this methodology for VCM design.

1. Introduction

Variable capacitance micromotor (VCM) is an important MEMS actuator [1], for which several applications are envisaged, amongst medical implants, optical systems, microrobotics, Aeronautics, and Space [2]. The electrostatic field of VCM is analyzed using FEM method due to difficulties encountered in calculating the electric field at the edges [3].

Less attention has been paid to optimization of the VCM design geometry. Exhaust algorithm based on 6% steps of each design parameter has been used in VCM optimization [4] for which every obtained combination made up of different variables was analyzed using FEM. The results however were not accurate, and the calculation time was reported to be long [5].

In this paper, a new method for VCM optimization is proposed based on Differential Evolution (DE). DE algorithm is a simple and extremely powerful evolutionary computation technique that solves real-value problems based on the principles of natural evolution [6]. DE uses a population of floating point encoded individuals and the operators of mutation,

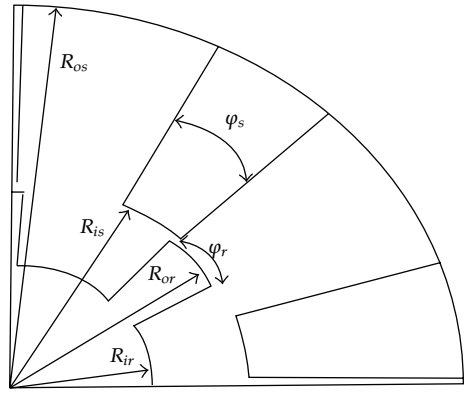

Figure 1: Micromotor configuration and geometrical parameters.

crossover, and selection to explore the solution space in search of a global optima [7]. Each individual or candidate solution is a vector that contains as many parameters as those of the problem dimensions. To get optimization shape of the micromotor, a combination of DE algorithm and FEM analysis is proposed. Fitness value is calculated using COMSOL3.4, and the DE algorithm is realized by MATLAB7.4.

The paper is organized as follows: Section 2 describes the torque calculation and excitation sequence of the VCM. Section 3 proposes a cost function and its control parameters in order to define the optimization problem. Detailed description of DE as well as its associated parameters tuning is presented in Section 4. Implementation of DE for geometric optimization and its comparison with the typical micromotor are discussed in Section 5. Finally, the conclusions are drawn in Section 6.

2. Variable Capacitance Micromotor

The cross-section of the micromotor being investigated in this study is shown in Figure 1. The rotor and stator are made from polysilicon film, and the medium between them is air. The modeled VCM has 8 stator electrodes grouped in 4 phases and 6 rotor poles and is excited by 100 V.

The stator and rotor have outer radius (R_{os} and R_{or}) of 100 μm and 50 μm, respectively. The gap between an aligned rotor and stator pole is 1.5 μm. The angular width of both stator and rotor electrodes, (φ_s and φ_r), is 18°, and the slot radius of the micromotor, R_{ir}, is 30 μm. The axial thickness of the rotor and stator is 2.2 μm [1].

2.1. The Mathematical Model of VCM

An electrostatic motor works based on the action of columbic forces in the gap between the stator and the rotor [8]. When voltage is applied between the rotor and stator electrodes the electrostatic force acts to align the electrodes. This type of micromotor demonstrates the concept of storing electrical energy within a variable stator-rotor capacitance [9].

Modeling the operation of the micromotor involves solving the electrostatic component of Maxwell's equation for force and therefore torque. Using finite element method,

the second-order partial differential equation is solved for the electric scalar potential V surrounding the stator and rotor poles of the micromotor [10]

$$-\varepsilon \nabla^2 V = \rho, \tag{2.1}$$

where ε is the electrical permittivity of the surrounding region and ρ is the charge density distribution on the rotor and stator. The electric field intensity E and electric flux density D can then be calculated from the following equations [10]:

$$\begin{aligned} E &= -\nabla V, \\ D &= \varepsilon \cdot E. \end{aligned} \tag{2.2}$$

Various methods can be used for computation of electrostatic forces in an electromechanical energy conversion device. The most commonly used methods are [11]

(1) stress tensor method,

(2) coenergy method.

The electrostatic force densities at every point on a closed contour located in the air gap of the machine can be calculated using Maxwell stress tensor method. However, the torque computed by this method does not take into account the torque ripples [12].

As far as the coenergy method is concerned, in order to obtain the electrostatic torque as a function of rotor position, the electrostatic energy must first be calculated. This energy is proportional to the capacitance between the stator and the rotor [13]. The stored energy in the electric field within the micromotor is obtained from the following equation:

$$W' = \frac{1}{2} C(\theta) \cdot V^2, \tag{2.3}$$

where C is the capacitance between the stator and the rotor with respect to the angular rotor position θ and V is the applied potential at the electrodes. The tangential component of the electrostatic force is calculated by differentiating total coenergy with respect to the position of the rotor for single phase excitation as follows [13]:

$$T(\theta) = \frac{\partial W'}{\partial \theta} = \frac{1}{2} \cdot \frac{\partial C(\theta)}{\partial \theta} \cdot V^2. \tag{2.4}$$

This method provides a relatively straightforward solution. In this study, a 2D finite element method has been used for analyzing the electrostatic field in the micromotor. Since we are dealing with an electrically linear system [14], the driving torque has been calculated per meter of the axial thickness which has then been multiplied by the actual axial thickness. The voltage distribution at rotor position of 15° has been illustrated in Figure 2. At all points, the electric field is perpendicular to the equipotential lines.

For energy calculation, one pair of stator electrodes is supplied with a constant voltage, while the other stator electrodes as well as the rotor are grounded. It is worth noting that the angular distance which the rotor must travel to move from alignment with one stator

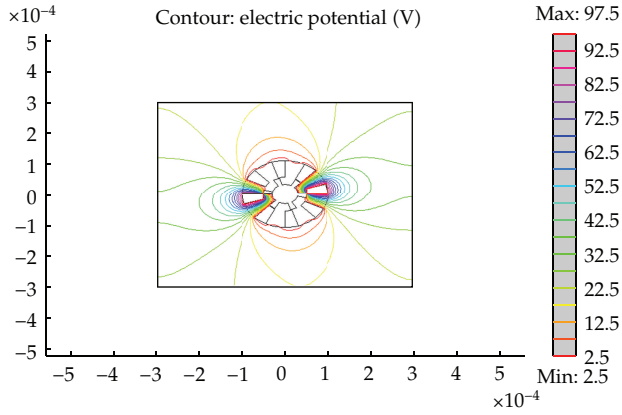

Figure 2: Geometry of the micromotor, showing the equipotential lines at $\theta = 15$ deg.

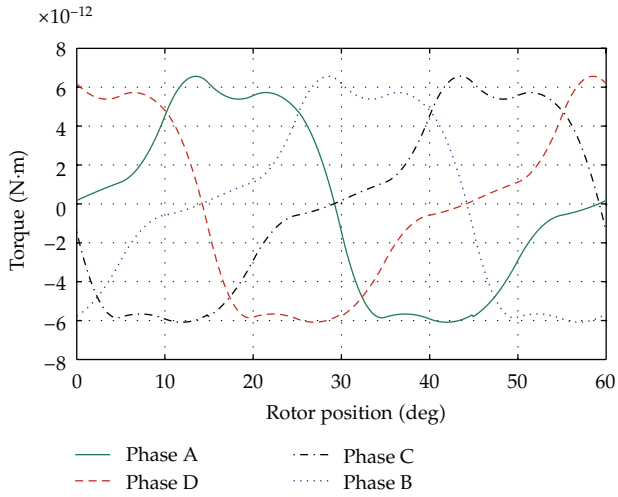

Figure 3: Torque-angle curves during one electric period for excitation schemes from *phase A* to *phase D*.

phase to the next is 60°. Once the electrodes are aligned, excitation to that pair of stator electrodes is switched off, and the subsequent pair is excited. At each rotor position, the stored energy in the electric field can be evaluated as a function of rotor position. The rotor moves through an angle of one degree between active stator electrodes. Hence, within each rotor pole pitch, 60 positions are obtained. In this work, a continuous curve is fitted to energy-angle points by the spline interpolation technique considered to be an effective tool for such data fitting [15]. The function of energy versus angle is then obtained from which the torque can be calculated as the partial derivative of energy versus the angular displacement. Figure 3 demonstrates torque profile versus rotor position for different phase excitations. Therefore, the torque obtained from the coenergy method is a function of rotor position and has average as well as ripple components. As mentioned earlier, in a 2-dimensional FEM, the driving torque is calculated per meter of the axial thickness. Since the electrostatic micromotor is a linear system, the torque has to be multiplied by the actual axial thickness.

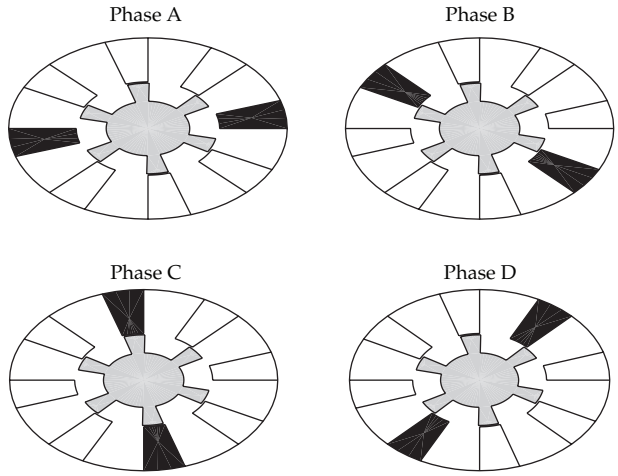

Figure 4: Symmetric excitations of a micromotor with 8 stator electrodes.

2.2. Excitation Sequence

A detailed knowledge of the distribution of forces in a micromechanical system such as a micromotor is of great importance for the analysis of such devices [16]. The forces exerted on the rotor act in three major orientations: axial, radial, and rotational. To maximize the torque, high tangential forces are desired, whereas axial and radial components should be minimized [16]. The excitation should therefore be applied symmetrically. Figure 4 illustrates the symmetrically excited sequence (excitation schemes from *Phase A* to *Phase D*) for the micromotor used in this work. The black electrodes in the figure are excited to 100 V, while the rotor and the other stator electrodes are grounded as stated previously.

Applying this excitation sequence, the torque-angle curves are obtained for each excitation scheme. By switching from one excitation scheme to another, at the crossover (see Figure 3), a smooth generated torque is achieved. Figure 5 shows the generated torque during one electric period for the optimal excitation sequence. As can be seen, the torque ripple is minimized in the resulting sequence.

3. Fitness Function and Geometric Variables of the Micromotor

Two key components of any optimization problem are choice and formulation of the appropriate objective function.

The objective function aims to maximize torque value and minimize the torque ripple in VCM design [5]. In FEM analysis, the torque is computed from the obtained nonlinear solution of the voltage using (2.1)–(2.4). The closed contour in the middle of the air gap is used as the path of integration.

In this work, two terms for the objective function are suggested. The first one, as indicated in (3.1), corresponds to the maximum torque value, for which the effective value of the torque in one electrical period is considered

$$T_{\text{rms}} = \sqrt{\frac{1}{\tau}\int_0^{\tau} T(\theta)^2 \cdot d\theta}, \tag{3.1}$$

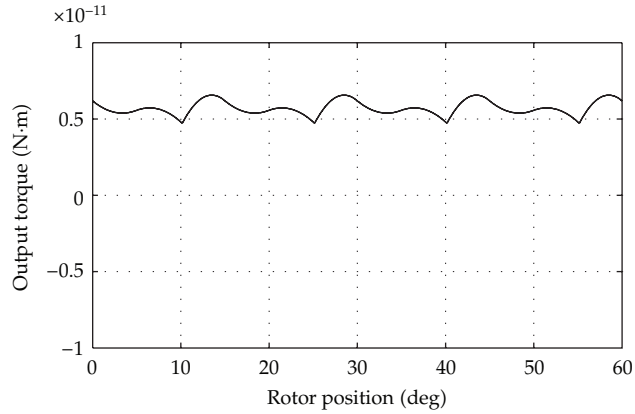

Figure 5: Output torque distribution.

where $T(\theta)$ is electrostatic torque at the rotor position θ and τ is the associated electrical period which is equal to $(2\pi/6)$ radian, or 60° here.

The second term in the objective function corresponds to the minimum torque ripple, for which the ripple factor (R.F) is defined as follows:

$$\text{R.F} = \frac{T_{\text{ac}}}{T_{\text{ave}}}, \tag{3.2}$$

where

$$\begin{aligned} T_{\text{av}} &= \frac{1}{\tau}\int_0^{\tau} T(\theta)\cdot d\theta, \\ T_{\text{ac}} &= \sqrt{\text{T}_{\text{rms}}^2 - \text{T}_{\text{ave}}^2}. \end{aligned} \tag{3.3}$$

T_{ave} and T_{ac} are average torque and AC component of torque in one electrical period, respectively.

The objective function, $f(x)$ defined in (3.4), which will satisfy both conditions of maximum torque and minimum ripple, is a weighted sum of both objective functions and needs to be minimized

$$f(x) = m\cdot\frac{T_{\text{rms0}}}{T_{\text{rms}}} + \frac{\text{R.F}}{\text{R.F}_0}, \tag{3.4}$$

where T_{rms0} and R.F_0 are, respectively, the effective torque and the ripple factor for the preliminary geometric parameters, that is, those of the typical micromotor. The weight factor for the torque term, m, is assumed to be 2 in this work.

The extent of the dependency of the objective function $f(x)$ on its variables cannot be expressed explicitly, while the value of the objective function can be computed by the FEM for each generated set of variables.

As far as the parameters considered for the optimization are concerned, several geometric parameters could be used as variables. Some of these are independent variables

Table 1: Design parameters and their boundary constraints.

Parameter	Symbol	Limits
Stator pole width	φ_s	$15^\circ < x_1 < 44^\circ$
Rotor pole width	φ_r	$15^\circ < x_2 < 59^\circ$
Rotor inner radius	R_{ir}	$20\,\mu\text{m} < x_3 < 50\,\mu\text{m}$

while others are dependent on other geometric parameters. Letting all parameters vary independently would make the optimization procedure too complex. However, a good convergence can be achieved if the optimization function parameters are taken to be independent [17]. The independent design parameters considered in this work are the stator pole width, the rotor pole width, and the rotor inner radius (see Figure 1). Air gap length is another independent design parameter which could have been selected here. It should be noted that the stator-rotor capacitance is inversely proportional to the distance between the stator and rotor and hence, the torque increases as the air gap length decreases. Therefore, the minimum air gap length of 0.003 mm is chosen in this work primarily due to fabrication constraints, and as such this term is not included for minimization.

There are some physical constraints which need to be considered. For instance, in real VCM, the rotor cannot overlap the stator, as indeed the stator poles cannot overlap each other. Table 1 shows the boundary constraints for these design parameters for the micrometer considered in this study.

4. Schemes and Mechanism of DE

4.1. Background

DE algorithm employs stochastic search technique and is one of later type amongst the evolutionary algorithms. At every generation G, DE maintains a population $P^{(G)}$ of N_p vectors of candidate solutions to the problem, which evolve throughout the optimization process to find global solutions [6]

$$P^{(G)} = \left[X_1^{(G)}, \ldots, X_{N_p}^{(G)}\right]. \tag{4.1}$$

The population size N_p does not change during the optimization process. The dimension of each vector of candidate solutions corresponds to the number of the decision parameters, D, to be optimized. Therefore,

$$X_i^{(G)} = \left[X_{1,i}^{(G)}, \ldots, X_{D,i}^{(G)}\right]^T, \quad i = 1, \ldots, N_p. \tag{4.2}$$

The optimization process includes three main operations: mutation, crossover, and selection. For any generation, each parameter vector of the current population becomes a target vector. For each target vector, the mutation operation produces a new parameter vector (called mutant vector), by adding the weighted difference between two randomly chosen vectors to a third (also randomly chosen) vector. By mixing the parameters of the mutant vector with those of the target vector, the crossover operation generates a new vector

(the trial vector). If the trial vector obtains a better fitness value than the target vector, then the trial vector replaces the target vector in the following generation.

DE has several reproduction schemes. The following one, denoted as DE1 here, is recommended by Storn and Price [18] as the first choice:

$$x'_{i,j}[k] = x_{i,j}[k] + K \cdot \left(x_{r3,j}[k] - x_{i,j}[k]\right) + F \cdot \left(x_{r1,j}[k] - x_{r2,j}[k]\right), \tag{4.3}$$

where $r_1 \neq r_2 \neq r_3 \neq i$ are integers randomly selected from 1 to population size. The parameters K and F are taken within the range of [0, 1]. If $x'_{i,j}[k]$ is found outside the range of $[x_j^{\min}, x_j^{\max}]$, it will then be fixed to the violated limit $x_j^{\max}$ or $x_j^{\min}$. Equation (4.3) demonstrates that, unlike other Evolutionary Algorithms (EAs) which rely on a predefined probability distribution function [6], the reproduction of DE is driven by the differences between randomly sampled pairs of individuals in the current population. This reproduction scheme, although simple, elegantly endows DE with the features of self-tuning and rotational invariance, which are crucial for an efficient EA scheme and have long been pursued in the EA community [19]. An even simpler DE scheme, denoted as DE2 here, can be derived from (4.3)

$$x'_{i,j}[k] = x_{i,j}[k] + K \cdot \left(x_{\text{best},j}[k] - x_{i,j}[k]\right) + F \cdot \left(x_{r1,j}[k] - x_{r2,j}[k]\right), \tag{4.4}$$

where $x_{\text{best},j}$ is the value of the jth control variable of the historical best individual (x_{best}) obtained from the former generations. DE2 can be viewed as a greedier version of DE1, because it exploits the information of the best individual to guide the search. This can speed up the convergence, because the way the best individual being utilized here is a kind of population acceleration [7]. At kth generation, a search point $x_i[k]$ is first accelerated by the term $K \times (x_{\text{best}}[k] - x_i[k])$, in (4.4), towards the historical best individual, x_{best}, and to some point that is located between $x_i[k]$ and x_{best}. This kind of acceleration forms a kind of contractive pressure and may cause premature convergence. But fortunately, the contractive pressure can be balanced by the diffuse pressure provided by the last term $F \times (x_{r1,\,j}[k] - x_{r2,j}[k])$ in (4.4), which diverts the search point in a random direction based on the difference between the randomly sampled $x_{r1}[k]$ and $x_{r2}[k]$. Therefore, the global searching ability can hopefully be maintained. So DE2 is used in this study.

4.2. Parameter Setting

There are mainly three parameters in DE, namely, K and F in (4.4) and the population size N_p. The proper setting of N_p is largely dependent on the size of the problem. Storn and Price [18] remarked that for real-world engineering, if the number of design parameters is larger than 2, the number of population members N_p should be at least 15 [7]. For problems with D variables, therefore, $N_p = 20 \times D$ will probably be more than adequate. Often N_p can be selected as small as $5D$, though optimal solutions using $N_p < 2 \times D$ should not be expected [18]. In this work, $N_p = 5 \times D$ is considered as a good choice for the first try. This can later be increased or decreased by discretion.

As mentioned before, K controls the strength of the contractive pressure, whereas F controls the strength of the diffusive pressure. The larger the value of K or F, the stronger is the contractive or diffusive pressure. High ratio of K to F may lead to premature

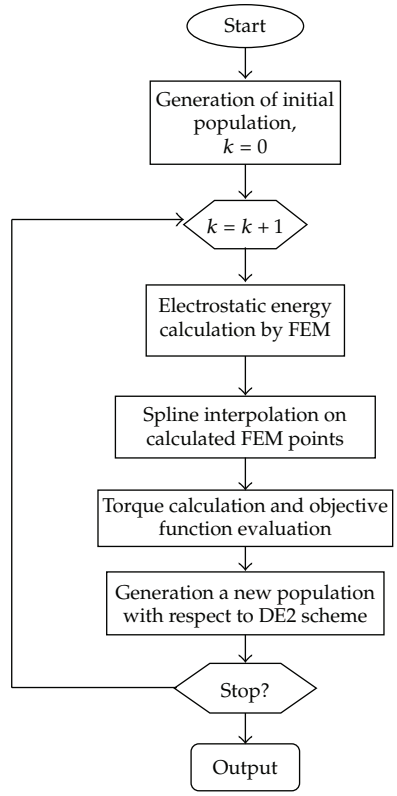

Figure 6: Flowchart for the micromotor optimization.

convergence, whereas low ratio of K to F may yield a too slow convergence. So, K and F must be coordinately set in order to achieve the best performance. However, based on the experimental studies [18], Price points out that choosing K randomly from the range of [0, 1] once per individual at each generation could be very effective. In this study, the recommended setting for the F is 0.7 and that for the K is selected randomly between 0 and 1.

In this study, a combination of DE algorithm and FEM analysis is employed to solve the VCM design optimization. Figure 6 illustrates the corresponding flowchart for this.

5. Simulation Results

In this work, optimization has been carried out in three cases: maximizing the torque, minimizing the ripple factor, and optimizing both of these simultaneously. The characteristics of the optimized and typical micromotor are compared by the following parameters:

$$\%\Delta T_{\text{rms}} = \frac{T_{\text{rms}} - T_{\text{rms0}}}{T_{\text{rms0}}} \times 100,$$
$$\%\Delta \text{R.F} = \frac{\text{R.F} - \text{R.F}_0}{\text{R.F}_0} \times 100, \tag{5.1}$$

Table 2: Geometric parameters for the typical VCM.

Parameter	Non-optimized VCM
Stator pole width φ_s	18°
Rotor pole width φ_r	18°
Rotor inner radius R_{ir}	30 μm
Ripple factor R.F$_0$	0.0393
Torque T_{rms}	5.6658 pN·m

where $\%\Delta T_{\text{rms}}$ and $\%\Delta$R.F are percentage changes of torque and ripple factor, respectively. The parameters of the typical micromotor introduced in Figure 1 are given in Table 2.

In order to investigate the performance of the DE algorithm proposed here, the VCM optimization is also carried out using GA with a large population size of 80 and rather large generation number of 100 with the crossover probability of 0.5 and mutation probability of 0.1.

As can be seen from the flowchart in Figure 6, to optimize a VCM with DE (or GA) and FEM, both must be adapted to function and operate in a coordinated manner. This means that to evaluate the objective function of a design parameter set (individual), the FEM package must be able to accept parameters generated by DE (or GA) in order to perform the FEM computation automatically and to return the value of the objective function to the optimization algorithm. All the algorithms are run in MATLAB7.4.0 in which COMSOL 3.4 is used for FEM analysis. This computation is carried out using a PC with Pentium 4 CPU Quad 2.83 GHz and 4 GB RAM.

5.1. Maximizing the Torque Value

Considering (3.1), the objective function for this exercise is

$$f(x) = \frac{T_{\text{rms0}}}{T_{\text{rms}}}. \tag{5.2}$$

As can be seen from the optimization results presented in Table 3, DE offers both shorter run-time and higher torque values compared with GA.

Figure 7 demonstrates the convergence curve of the objective function against the iteration number for the DE algorithm. It has reached a minimum of about 0.94 after 45 iterations in almost 30 hours runtime. Figure 8 shows the graphs of torque versus angle for the typical and a DE-optimized micromotor. Despite increasing the ripple factor, the optimization has increased the torque value of the VCM by more than 6.5%.

5.2. Minimizing the Torque Ripple

Considering (3.2), the objective function for the ripple factor minimization can be defined by the following formula:

$$f(x) = \frac{\text{R.F}}{\text{R.F}_0}. \tag{5.3}$$

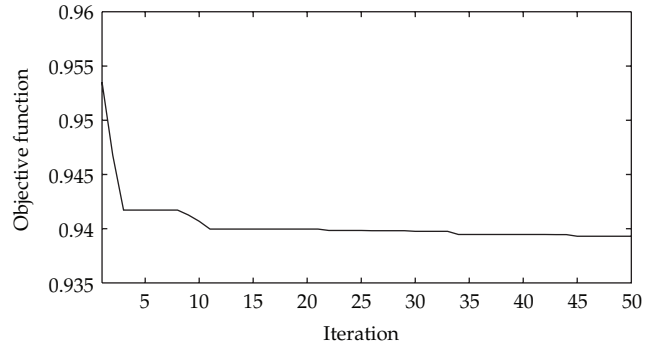

Figure 7: Convergence curves of DE for "torque optimization."

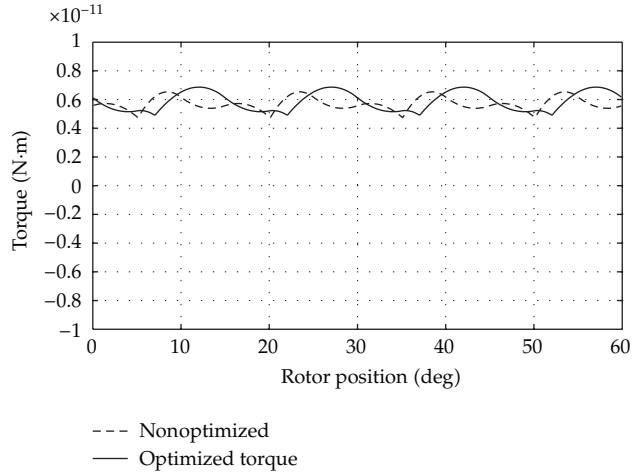

Figure 8: Torque profile before and after "torque optimization."

Table 3: Results of "torque optimization" for VCM geometric parameters.

Parameter	DE	GA
Stator pole width φ_s	30.5505°	27.4745°
Rotor pole width φ_r	16.5018°	20.5602°
Rotor inner radius R_{ir}	20.336 μm	25.0634 μm
Ripple factor R.F$_0$	0.1347	0.0418
Torque T_{rms}	6.0366 pN·m	5.9860 pN·m
Objective function $f(x)$	0.9393	0.9453
Population size N_p	30	80
Number of iteration G	50	100
Run time	30 hours	160 hours

The geometric parameters for optimized micromotors using DE and GA are expressed in Table 4.

It can be observed that DE yields improved results in terms of both optimization elapsed time (due to smaller population size and less number of iterations) and ripple factor.

Table 4: Results of "ripple optimization" for VCM geometric parameters.

Parameter	DE	GA
Stator pole width φ_s	21.693°	28.1454°
Rotor pole width φ_r	23.209°	23.9437°
Rotor inner radius R_{ir}	45.8831 μm	27.2193 μm
Ripple factor R.F$_0$	0.000306	0.0067
Torque T_{rms}	4.7498 pN·m	5.810 pN·m
Objective function $f(x)$	0.00779	0.17003
Population size N_p	30	80
Number of iteration G	100	100
Run time	60 hours	160 hours

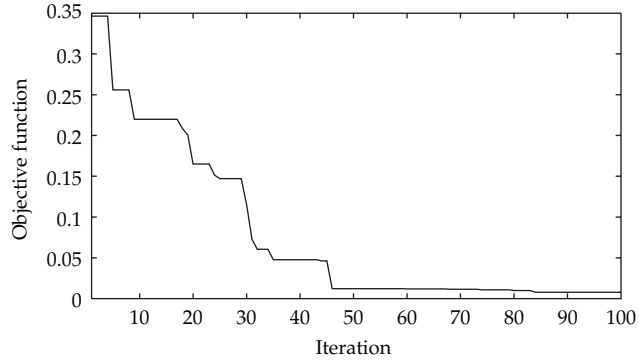

Figure 9: Convergence curves of DE for "ripple optimization."

The convergence process for the DE algorithm is illustrated in Figure 9. The torque angle curves for the typical and optimized VCM are compared in Figure 10, which indicates a substantial decrease in the ripple factor (almost 95%), while the value of the torque has decreased.

5.3. Simultaneous Torque Value Maximization and Torque Ripple Minimization

The objective function for simultaneous torque value maximization and torque value minimization is defined in (3.4). The geometric parameters for this aim using DE and GA are expressed in Table 5.

Again, the optimization results presented in Table 5 indicate that DE offers both shorter run-time and higher torque values compared with GA.

Figure 11 shows the convergence process using DE algorithm obtained after 40 iterations. The corresponding torque angle curve with a 2.5% increase in the torque value and 82% decrease in the ripple factor is shown in Figure 12.

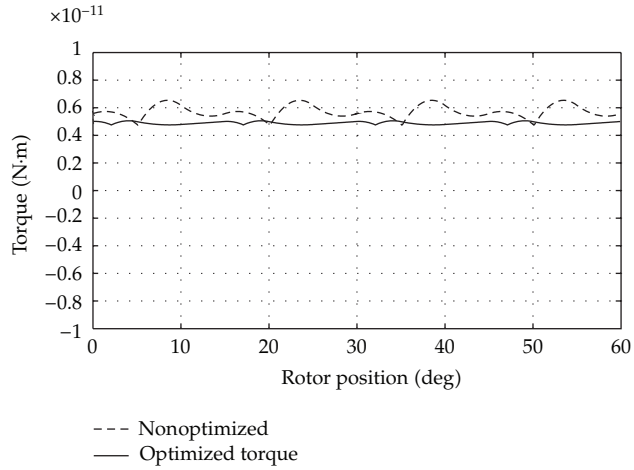

Figure 10: Torque profile before and after "ripple optimization."

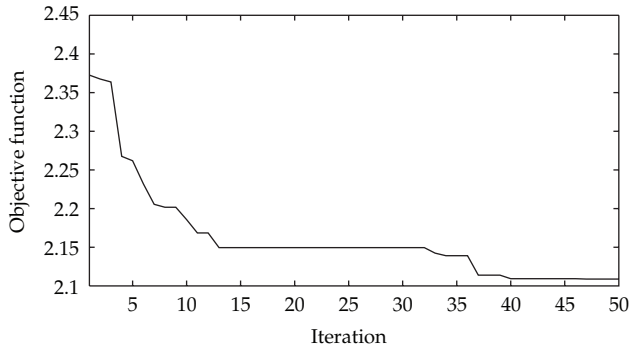

Figure 11: Convergence curves of DE for "torque and ripple optimization."

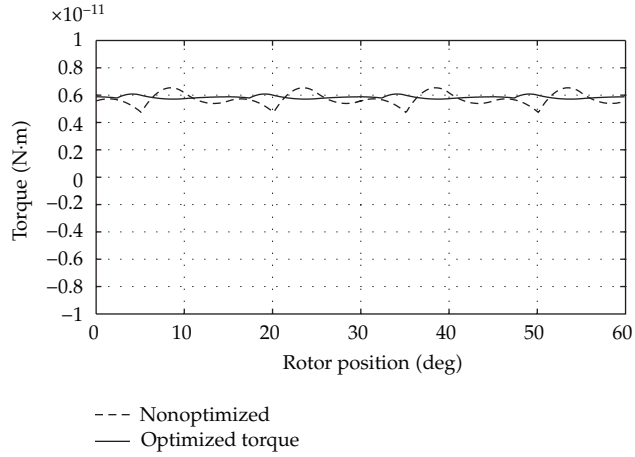

Figure 12: Torque profile before and after "torque and ripple optimization."

Table 5: DE Results of "torque and ripple optimization" for VCM geometric parameters.

Parameter	DE	GA
Stator pole width φ_s	27.9317°	24.0924
Rotor pole width φ_r	23.9762°	27.6354
Rotor inner radius R_{ir}	23.1135 μm	37.1227
Ripple factor R.F$_0$	0.0061	0.0111
Torque T_{rms}	5.801 pN·m	5.6455 pN·m
Objective function $f(x)$	2.1087	2.29
Population size N_p	30	80
Number of iteration G	50	100
Run time	30 hours	160 hours

6. Conclusion

In this paper, following description of the principle operations for a VCM, a combined application of DE with FEM analysis for torque calculations is explained. Using spline interpolation, a continuous curve is fitted to the energy-angle points, from which torque is then calculated by differentiation. After selecting the appropriate independent geometric parameters for the micromotor optimization, a suitable objective function is presented. Using DE, as a powerful evolutionary computation technique, a typical VCM is optimized in conjunction with FEM for which all the algorithms are implemented in MATLAB environment. The proposed method was verified on a VCM with 8 poles at the stator and 6 poles at the rotor.

The results show enhanced torque value and decreased torque ripple when compared with the typical micromotor, indicating improved efficiency in the VCM performance. When compared with GA, DE scheme reaches the optimal solutions faster, with less objective function. Hence, this approach could well be applied for optimizing the performance of other MEMS devices.

References

[1] S. F. Bart, M. Mehregany, L. S. Tavrow, J. H. Lang, and S. D. Senturia, "Electric micromotor dynamics," *IEEE Transactions on Electron Devices*, vol. 39, no. 3, pp. 566–575, 1992.

[2] T. C. Neugebauer, D. J. Perreault, J. H. Lang, and C. Livermore, "A Six-Phase Multilevel Inverter for MEMS Electrostatic Induction Micromotors," *IEEE Transactions on Circuits and Systems II*, vol. 51, no. 2, pp. 49–56, 2004.

[3] W. Zhang, G. Meng, and H. Li, "Electrostatic micromotor and its reliability," *Microelectronics Reliability*, vol. 45, no. 7-8, pp. 1230–1242, 2005.

[4] V. Behjat and A. Vahedi, "Minimizing the torque ripple of variable capacitance electrostatic micromotors," *Journal of Electrostatics*, vol. 64, no. 6, pp. 361–367, 2006.

[5] T. B. Johansson, M. Van Dessel, R. Belmans, and W. Geysen, "Technique for finding the optimum geometry of electrostatic micromotors," *IEEE Transactions on Industry Applications*, vol. 30, no. 4, pp. 912–919, 1994.

[6] R. Sarker, M. Mohammadian, and X. Ya, Eds., *Evolutionary Optimization*, International Series in Operations Research & Management Science, 48, Kluwer Academic Publishers, Boston, Mass, USA, 2002.

[7] K. V. Price, R. M. Storn, and J. A. Lampinen, *Differential Evolution: A Practical Approach to Global Optimization*, Natural Computing Series, Springer, Berlin, Germany, 2005.

[8] W. K. S. Pao, W. S. H. Wong, and A. M. K. Lai, "An explicit drive algorithm for aiding the design of firing sequence in side-drive micromotor," *Communications in Numerical Methods in Engineering*, vol. 24, no. 12, pp. 2131–2136, 2008.

[9] S. S. Irudayaraj and A. Emadi, "Micromachines: principles of operation, dynamics, and control," in *Proceedings of IEEE International Conference on Electric Machines and Drives*, pp. 1108–1115, May 2005.

[10] F. Delfino and M. Rossi, "A new FEM approach for field and torque simulation of electrostatic microactuators," *Journal of Microelectromechanical Systems*, vol. 11, no. 4, pp. 362–371, 2002.

[11] L. S. Fan, YU. C. Tai, and R. S. Muller, "IC-processed electrostatic micro-motors," in *Proceedings of IEEE International Electron Devices Meeting*, pp. 666–669, December 1988.

[12] A. Jindal, M. Krishnamurthy, and B. Fahimi, "Modeling and analysis of a micro variable capacitance electromechanical energy converter," in *Proceedings of the International Symposium on Power Electronics, Electrical Drives, Automation and Motion (SPEEDAM '06)*, pp. 358–363, May 2006.

[13] S. Wiak, P. Di Barba, and A. Savini, "3-D computer aided analysis of the 'Berkeley' electrostatic micromotor," *IEEE Transactions on Magnetics*, vol. 31, no. 3, pp. 2108–2111, 1995.

[14] V. Behjat and A. Vahedi, "Analysis and optimization of MEMS electrostatic microactuator," in *Proceedings of the 3rd International Conference of Young Scientists on Perspective Technologies and Methods in MEMS Design (MEMSTECH '07)*, pp. 20–25, May 2007.

[15] L. L. Schumaker, *Spline Functions: Basic Theory*, Cambridge Mathematical Library, chapter 1, Cambridge University Press, Cambridge, UK, 3rd edition, 2007.

[16] N. G. Milne, S. J. E. Yang, A. J. Sangster, H. Ziad, and S. Spirkovitch, "Determination of the forces present in an electrostatic micromotor," in *Proceedings of IEEE International Conference on Electrical Machines and Drives*, pp. 9–14, 1993.

[17] R. L. Haupt and D. H. Werner, *Genetic Algorithms in Electromagnetics*, IEEE Press, New York, NY, USA, 2007.

[18] R. Storn and K.V Price, "Differential evolution—a simple and efficient adaptive scheme for global optimization over continuous spaces," Tech. Rep. TR-95-012, International Computational Science Institute, Berkley, Mich, USA, 1995.

[19] D. Corne, M. Dorigo, and F. Glover, *New Ideas in Optimization*, McGraw-Hill, London, UK, 1999.